

# DEVELOPMENT OF TWO-DIMENSIONAL NUMERICAL WAVE FLUME FOR WAVE INTERACTION WITH RUBBLE MOUND BREAKWATERS

Peter Troch<sup>1</sup>, Julien De Rouck<sup>2</sup>

## Abstract

The numerical wave flume VOFbreak<sup>2</sup> for simulation of wave interaction with a rubble mound breakwater is presented. The key innovations are a porous flow model and wave boundary conditions. The porous flow is implemented using a Forchheimer model. At the boundaries waves are generated using a combined wave generation-absorption technique and are absorbed using a numerical sponge layer.

## 1 Introduction

A 2D numerical model for the simulation of free surface breaking waves at permeable coastal structures is developed at the Department. This numerical wave flume VOFbreak<sup>2</sup> aims at a better description of the wave-induced flows and pressures at porous structures, resulting in a better design (tool) of coastal structures. Special attention is paid to the application of the model to wave interaction with a rubble-mound breakwater. Fig. 1 shows a snapshot of the simulation of a typical numerical wave flume set-up where waves interact with the porous breakwater.

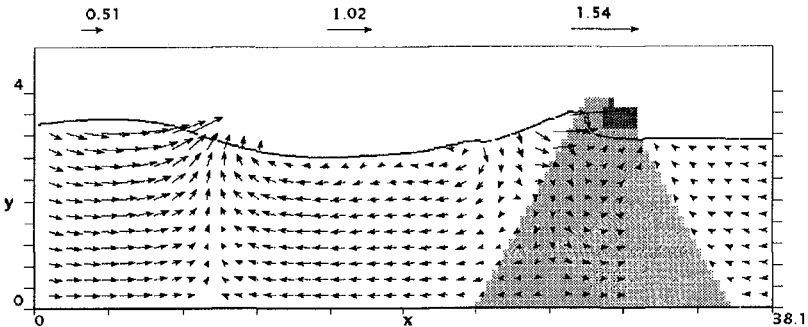


Fig. 1. Snapshot of a typical numerical simulation of wave interaction with a rubble mound breakwater using VOFbreak<sup>2</sup>.

<sup>1</sup> Research Assistant, Dept. Of Civil Engineering, University of Gent, Technologiepark 9, B-9052 Gent, Belgium. Email: PeterB.Troch@rug.ac.be.

<sup>2</sup> Professor, Dept. Of Civil Eng., University of Gent, Technologiepark 9, B-9052 Gent, Belgium.

First the underlying mathematical and numerical models of VOFbreak<sup>2</sup> are presented briefly. Secondly the key innovations in the numerical wave flume that are necessary for simulation of wave interaction with permeable rubble mound structures are discussed in more detail: a porous flow model and wave boundary conditions. Finally an example application illustrates the model features.

## 2 Numerical wave flume VOFbreak<sup>2</sup>

### 2.1 Mathematical model

The numerical wave flume VOFbreak<sup>2</sup>, VOF-algorithm for breaking waves on breakwaters, is based on the original SOLA-VOF code (Nichols et al., 1980) capable to compute free surface flow when the fluid domain becomes multiply connected. Incompressible Newtonian fluid with uniform density is assumed in the vertical plane (two-dimensional), governed by the Navier-Stokes equations:

$$\frac{\partial u}{\partial t} + u \frac{\partial u}{\partial x} + v \frac{\partial u}{\partial y} = -\frac{1}{\rho} \frac{\partial p}{\partial x} + \nu \left( \frac{\partial^2 u}{\partial x^2} + \frac{\partial^2 u}{\partial y^2} \right) + g_x \quad (1)$$

$$\frac{\partial v}{\partial t} + u \frac{\partial v}{\partial x} + v \frac{\partial v}{\partial y} = -\frac{1}{\rho} \frac{\partial p}{\partial y} + \nu \left( \frac{\partial^2 v}{\partial x^2} + \frac{\partial^2 v}{\partial y^2} \right) + g_y \quad (2)$$

and the continuity equation:

$$\frac{\partial u}{\partial x} + \frac{\partial v}{\partial y} = 0 \quad (3)$$

where  $t$  (s) is time,  $u$  and  $v$  (m/s) are the velocity components in  $x$  and  $y$  direction respectively.,  $p$  (N/m<sup>2</sup>) is pressure, and  $g_x$ ,  $g_y$  (m/s<sup>2</sup>) are horizontal and vertical gravity components respectively,  $\rho$  (kg/m<sup>3</sup>) is the density of the water,  $\nu$  (m<sup>2</sup>/s) is the kinematic coefficient of viscosity.

The free surface is described by introducing a function  $F(x, y, t)$  that represents the fractional volume of fluid in the mesh cells. The volume of fluid evolution equation (4) expresses that the volume fraction  $F$  moves with the fluid:

$$\frac{\partial F}{\partial t} + u \frac{\partial F}{\partial x} + v \frac{\partial F}{\partial y} = 0 \quad (4)$$

### 2.2 Numerical model

Finite difference solutions of the four unknowns  $u$ ,  $v$ ,  $p$  and  $F$ , are obtained on an Eulerian rectangular mesh in a Cartesian co-ordinate system  $(x, y)$ .

The Navier-Stokes equations (1)-(2) are discretised using a combined FTCS/upwind scheme. As a result, explicit approximations of the Navier-Stokes equations are used to compute the first guess for new-time-level velocities.

To satisfy the continuity equation (3), i.e. to obtain a divergence free velocity field, the pressure-velocity iteration is used. It is a variant of the Newton-Raphson relaxation technique applied to the pressure Poisson equation for incompressible flow. Using this method, pressures are iteratively adjusted in each cell and velocity changes induced by each pressure change are added to the velocities computed out of the Navier-Stokes equations.

Finally, the volume of fluid function  $F$ , defining the fluid regions, is updated using the donor-acceptor flux approximation for the calculation of fluxes from a donor cell to an acceptor cell. A unit value of  $F$  corresponds to a full cell, while a zero value indicates an empty cell. Cells with values between zero and one and having at least one empty neighbour cell contain a free surface. A line is constructed in each surface cell with the correct calculated surface slope and correct amount of fluid lying on the fluid size, and is used as an approximation to the actual free surface.

### 2.3 Code portability

The code VOFbreak<sup>2</sup> is based on SOLA-VOF (Nichols et al., 1980) and includes some selected improvements from its successor code NASA-VOF2D (Torrey et al., 1985). These are mainly a numerical defoamer technique preventing non-physical voids inside the fluid to appear, and fixes in the donor-acceptor algorithm.

The code is implemented on a UNIX workstation using ANSI C, providing general computer compatibility, and providing a flexible code structure for adaptations with little effort. A series of post-processing tools has been developed, using Tcl/Tk (Ousterhout, 1994), for the visualisation, processing and interpretation of the computed results. Numerical instrumentation for the acquisition of relevant phenomena (wave height, run-up level, pore pressure, surface elevation, ...) is included for easy access to calculated data.

## 3 Porous flow model

A breakwater is composed of a porous core, and porous filter and armour layers, which are made using coarse granular material. For a simulation of wave induced porous flow, this material is considered homogeneous and isotropic within areas where one characteristic porosity  $n$  and one characteristic diameter  $d$  are assigned. Following assumptions are used for porous flow:

- The discharge (or filter) velocity  $u$ , in  $x$  direction, is replaced by the pore (seepage) velocity  $u_p = u/n$ ; regarded as a macroscopic quantity, i.e. the discharge velocity is averaged over a cross sectional area consisting of a mixture of material and voids. The porosity  $n$  of the cell material is defined as the ratio between the volume of the pores and the total volume.
- The  $F$ -function is now considered as the fraction of maximum volume of fluid in a cell.
- The Forchheimer resistance terms replace the viscosity terms in the Navier-Stokes equations, these are expressed by the hydraulic gradient  $I$  (-), e.g. in  $x$  direction (Burcharth et al., 1995):

$$I = -\frac{1}{\rho g} \frac{\partial p}{\partial x} = au + bu|u| + c \frac{\partial u}{\partial t} \quad (5)$$

where the Forchheimer coefficients  $a$  and  $b$  take the form:

$$a = \alpha \frac{(1-n)^2}{n^3} \frac{\nu}{gd^2} \quad (6)$$

$$b = \beta \frac{1-n}{n^3} \frac{1}{gd} \quad (7)$$

and the inertia coefficient  $c$  takes the form:

$$c = \frac{n+(1-n)C_m}{g}, \text{ where } C_m = 1 + C_A \quad (8)$$

where  $\alpha$  and  $\beta$  are dimensionless constants,  $\nu$  ( $m^2/s$ ) is the kinematic coefficient of viscosity,  $g$  ( $m/s^2$ ) is the gravitational acceleration,  $n$  (-) is the porosity,  $d$  (m) is a characteristic stone diameter,  $C_A$  (-) is the added mass coefficient.

The linear term  $au$  in equation (5) constitutes the contribution from the laminar flow. The non-linear term,  $bu|u|$ , represents the fully turbulent flow contribution. The term  $c\partial u/\partial t$ , taking into account the inertia forces connected with the local accelerations  $\partial u/\partial t$ , represents the resistance of the porous medium to accelerate the water.

A verification of the implementation of the one-dimensional porous flow in steady state flow conditions has been carried out by comparing numerical calculated results to experimental measurements (Troch, 1997).

## 4 Wave Boundary Conditions

### 4.1 Introduction

In Fig. 2 a conventional numerical wave flume set-up is given. Waves are generated at the left boundary of the computational domain and propagate towards a rubble mound breakwater positioned near the other boundary. The incident waves interact with the porous breakwater causing transmitted and reflected waves to propagate towards the boundaries. At the boundaries, an 'open boundary' or 'absorbing boundary' condition is required, allowing the transmitted and reflected waves to leave the computational domain without disturbing the interaction of the incident waves with the breakwater.

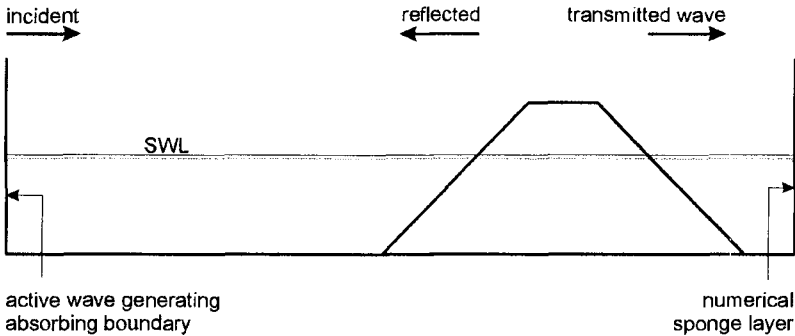


*Fig. 2. Conventional numerical wave flume set-up with boundary conditions for the study of wave interaction with porous rubble mound breakwater.*

The numerical problem is similar to the wave absorption problems in a physical wave flume. Therefore in principle the same solutions could be applied in the numerical flume. Schäffer and Klopman (1997) give an overview of the basic concepts of wave absorption in physical wave flumes.

However in order to increase the computational efficiency of the calculations a number of constraints are present. These are very important in the final choice of the numerical wave boundary conditions. A very important constraint is that the length of the numerical wave flume should be as short as possible for reasonable CPU time. Therefore the numerical wave flume requires a relatively short foreshore (1 or 2 wavelengths), and a very short lee-side (maximum 1 wavelength). The wave absorption techniques need to perform in these conditions. Also an efficient and simple technique that absorbs waves numerically might be more favourable than the numerical simulation of the physical behaviour of e.g. a progressive wave absorber.

The generation of incident waves is implemented in VOFbreak<sup>2</sup> using boundary generation. Any wave theory can be used to provide the surface elevation  $\eta(x_0, t)$  and the velocity components  $u(x_0, z, t)$  and  $v(x_0, z, t)$  at the left boundary ( $x_0=0$ ). For the simulations in this paper linear wave theory is used. Another efficient wave generation technique is source generation (Brorsen and Larsen, 1987) where the volume from the incident wave is added inside the computational domain. The advantage of this latter method is that the generation of the incident waves is not disturbed by the reflected waves. The disadvantage is that the length of the computational domain is considerably increased because a relatively long absorption layer is required for absorption of the reflected waves at the boundaries. Iwata et al. (1996) have successfully implemented the source generation technique in a SOLA-VOF model. The absorption layers required up to 6 wavelengths for sufficient wave absorption.

The wave absorption generally is divided into active systems and passive systems. An active system provides an active response to the waves; a passive system damps (mostly by energy dissipation) the wave motion. For this application, the transmitted waves are passively absorbed using an efficient numerical sponge layer technique

from Larsen and Dancy (1983). This passive absorption system is discussed in more detail in the next section. The reflected waves are actively absorbed at the wave-generating boundary using an active wave absorption technique. A detailed discussion of the active system performance in the VOFbreak<sup>2</sup> model is described in Troch and De Rouck (1998).

#### 4.2 Numerical Sponge Layer

Larsen and Dancy (1983) presented an efficient numerical passive wave absorber for use in short wave models. This technique is implemented into the VOFbreak<sup>2</sup> model. It has been chosen because of its very elegant and simple use. An absorption function  $a(x)$  is applied on velocities and elevation in a numerical sponge layer with length  $x_s$ , Fig. 3. The absorption function at the start of the sponge layer equals 1 and gradually decreases to 0 near the end of the sponge layer. The sponge layer is located at the closed end of the wave flume. Only a limited number of grid cells is required for absorption of the wave.

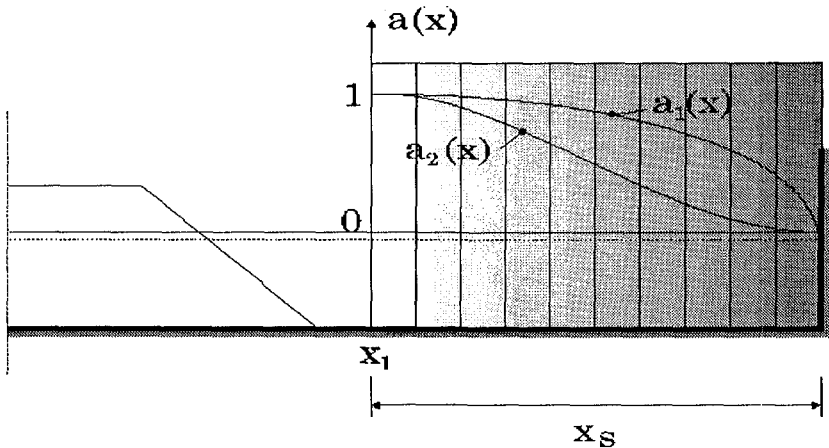


*Fig. 3. Numerical sponge layer with width  $x_s$  placed at the end of the numerical wave flume. The two absorption functions  $a(x)$  are plotted inside the sponge layer.*

Two simple absorption functions have been used for testing the performance of the sponge layer technique: an elliptic function  $a_1(x)$  (equation (9)) and a cosine function  $a_2(x)$  (equation (10)):

$$a_1(x) = \sqrt{1 - \left(\frac{x - x_1}{x_s}\right)^2} \quad (9)$$

$$a_2(x) = 0.5 \left( 1 + \cos\left(\frac{\pi}{x_s}(x - x_1)\right) \right) \quad (10)$$

The absorption function is applied on the calculated velocity components in the cells of the sponge layer after each time step calculation. In the present simulations no attempt has been made to apply the absorption function on surface elevations. The surface elevation is not a direct unknown of the system of differential equations (1)-(4), but is derived from the F function in each column of cells. A damping of the surface elevation means deleting volume fractions and doing this without adjusting the pressure consequently in each cell would lead to non-converging solutions.

The performance of the two types of sponge layer has been tested by deriving reflection ( $K_r$ ) and transmission ( $K_t$ ) coefficients from a sponge layer located inside the numerical wave flume. The water depth  $d = 0.40$  m, the wave height  $H = 0.02$  m, the wave period  $T = 1.60$  s. The width of the sponge layer varied between 40% and 60% of the wavelength  $L = 2.84$  m. The results are summarized in Table 1.

	$x_s/L$ [-]	$K_r$ [%]	$K_t$ [%]
a1	0.40	27	7
a1	0.60	21	3
a2	0.60	33	1

**Table 1.** Reflection ( $K_r$ ) and transmission ( $K_t$ ) coefficients from sponge layer performance tests.

The elliptic absorption function  $a_1$  with a length  $x_s = 0.40L$  still has a considerable reflection coefficient of 27% and transmission coefficient of 7%. Increasing the sponge layer width to  $0.60L$  decreases reflection to about 20% and almost no transmission (3%). In comparison the cosine absorption function with a width of  $0.60L$  still shows 33% reflection but no transmission.

It is concluded from these simple performance tests that the elliptic  $a_1$  type function performs better than the cosine  $a_2$  type. A slightly larger width  $x_s$  of the sponge layer would be required for practical purposes: it is suggested to use a width between  $0.60L$  and  $1.0L$ . It is noted that the absorption function not necessarily should equal 0 at the end of the sponge layer, it is more important to have a gradually decrease causing least reflection of the waves. In order to decrease the number of cells in the sponge layer it might be preferable to increase gradually the cell width towards the boundary.

There are other solutions available to obtain an open boundary.

- The well-known radiation boundary (also referred to as the Sommerfeld or the weakly reflecting boundary (used e.g. in the SKYLLA model, van der Meer et al., 1992) is another efficient solution. This method might become elaborate when working with irregular waves.

- Modelling of a spending beach with a mild slope (1:10 or more) would require a long distance to be modelled. This solution is not efficient for use in a numerical flume.
- Modelling of a physical progressive passive wave absorber with decreasing porosity would need a comprehensive description of geometry, porous flow characteristics, etc. Also for the physical performance of this solution it is required to go through the full model equations resulting in a longer calculation time.
- An active wave absorption system (see next section for more details) provides an active response at the boundary to the transmitted wave leaving the domain. It generally is used at the wave generating boundary in combined wave generating-absorbing mode, but the system is usable for wave absorption only. This solution is very elegant, but more complicated to implement in the numerical model than the sponge layer.

#### 4.3 Active wave absorption system

The active wave generating-absorbing system implemented in the numerical wave flume is based on the AWASYS system (Frigaard and Christensen, 1994) from Aalborg University. The AWASYS system originally is a surface elevation based system to be used in a physical wave flume with two conventional wave height meters. The system for VOFbreak<sup>2</sup> is based on a velocity meter based system because velocities are readily (or computationally cheap) available from the computations. Hald and Frigaard (1996) show that the performance (i.e. the absorption characteristics) of both elevations and velocities systems is similar.

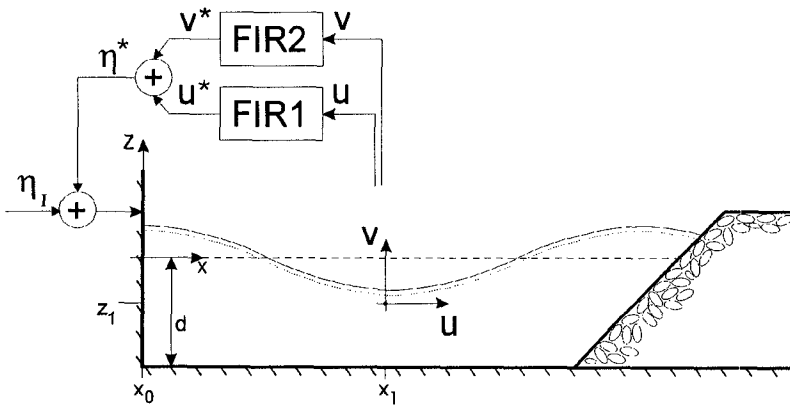


**Fig 4.** Definition sketch of the numerical wave flume set-up and the principle of the active wave generating-absorbing boundary condition.



The principle of the active wave generating-absorbing system requires two steps. First an on-line detection of the reflected wave field is performed using a set of spatially co-located velocities ( $u$ ,  $v$ ). Secondly the wave generator has to generate the incident wave and an additional wave which cancels out the reflected wave propagating towards the boundary. Fig. 4 shows schematically the principle of the system. The correction signal  $\eta^*$  that cancels out the reflected wave, is determined from superposition of the two filtered velocity signals  $u^*+v^*$ . The digital Finite Impulse Response (FIR) filters are operated using a time-domain discrete convolution of the velocities ( $u$ ,  $v$ ) and the impulse response  $h^i$ , where  $i = u$  or  $v$ ; e.g. for the  $u$  velocity component:

$$u^*[n] = \sum_{j=0}^{J-1} h^u[j] \cdot u[n-j] \quad (11)$$

where  $J$  is the number of filter coefficients, and  $u^*[n] = u^*(n \cdot \Delta t_f)$  is the filter output at time  $t = n \cdot \Delta t_f$ , where  $\Delta t_f$  is the filter time interval.

Having outlined the principle of the active wave generation-absorption, the only task remains the design of the corresponding frequency response function  $H(f)$  of the filters from where the impulse response function  $h(t)$  is easily derived using inverse Fourier Transform. The theoretical and practical design of the frequency response function for use in a numerical wave flume is described in Troch and De Rouck, 1998.

## 5 Example application

To demonstrate the possibilities of the VOFbreak<sup>2</sup> model for coastal engineering applications, a simulation of regular waves attacking a conventional rubble mound breakwater with permeable homogeneous core, is given. Fig. 5 is a snapshot during wave run-up and wave run-down respectively, and shows the induced velocity field in front of the breakwater and inside the breakwater core. From the zoomed slope area (Fig. 6) it is seen clearly that the occurring flow pattern cannot be reduced to one dimension. Both infiltration and seepage of pore water arise simultaneously along the slope.

Therefore this type of 2D model is better equipped to simulate wave-structure interaction than one-dimensional models. The model also gives a better insight in the wave interaction dynamics at the breakwater and may be helpful to assist to improve design guidelines.

The numerical model is verified with both physical model data and prototype data. This latter validation is unique world-wide by using the Zeebrugge breakwater (Belgium) prototype wave and pressure data (Troch et al., 1996). Validation results will help to improve further developments of the numerical wave flume.

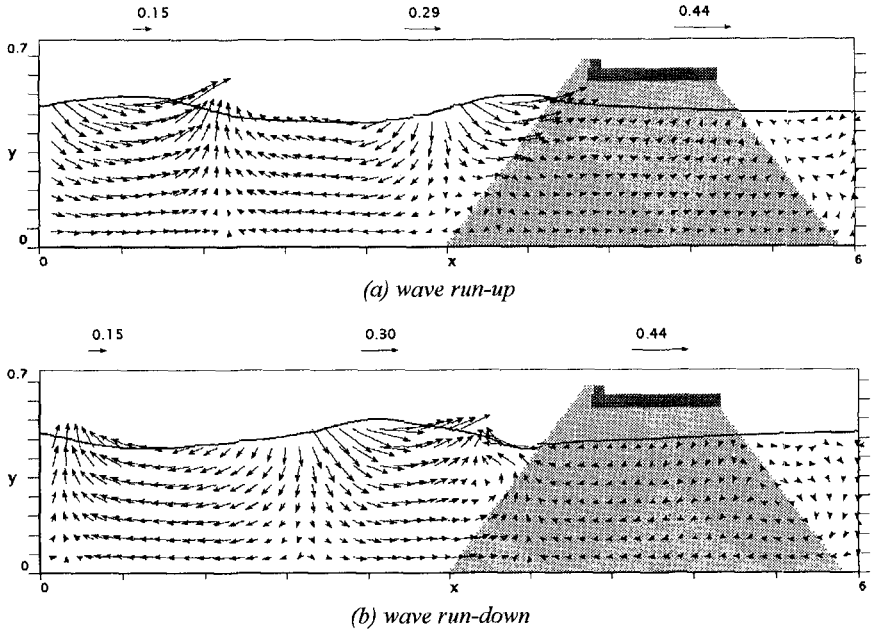


**Fig. 5.** Regular incident waves on and in permeable breakwater. Snapshot of calculated free surface location and velocity field during wave run-up (a - top) and run-down (b - bottom).

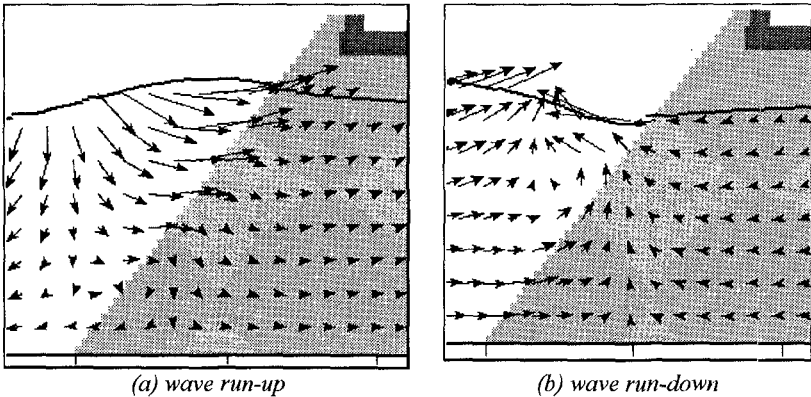


**Fig. 6.** Zoom of calculated free surface location and velocity field at the breakwater slope during wave run-up (a - left) and run-down (b - right).

## Acknowledgements

The development of this work originated during the EC MAST2 project MAS02-CT92-0023. The financial support of EC is greatly acknowledged. Discussions with Ass. Prof. Michael Brorsen and Ass. Prof. Peter Frigaard from Aalborg University, Denmark, on wave boundary modelling are very much appreciated.

## References

- Brorsen M. and Larsen J., 1987. Source Generation of nonlinear gravity waves with boundary integral equation method. *Coastal Eng.*, Vol 11, pp. 93-113.
- Burcharth H.F., Andersen O.H., 1995. On the one-dimensional steady and unsteady porous flow equations. *Coastal Eng.*, 24: 233-257.
- Frigaard P. and Christensen M., 1994. An absorbing wave-maker based on digital filters. In: *Proceedings, 24<sup>th</sup> International Conference on Coastal Engineering, Kobe, Japan, Vol.1, pp. 168-180.*
- Hald T. and Frigaard P., 1996. Performance of active wave absorption systems – comparison of wave gauge and velocity meter based systems. In: *Proceedings 2<sup>nd</sup> International Conference on Coastal, Ports and Marine Structures. ICOPMAS, Tehran, Iran.*
- Iwata K., Kawasaki K., Kim D., 1996. Breaking limit, breaking and post-breaking wave deformation due to submerged structures. In: *Proceedings 25<sup>th</sup> International Conference on Coastal Engineering, Orlando, USA, Vol.3, pp. 2338-2351.*
- Larsen J. and Dancy H., 1983. Open boundaries in short wave simulations -- a new approach. *Coastal Eng.*, Vol. 7, pp. 285-297.
- Nichols B.D., Hirt C.W., Hotchkiss R.S, 1980. SOLA-VOF: a solution algorithm for transient fluid flow with multiple free boundaries. Report LA-8355, Los Alamos, California, USA.
- Ousterhout J.K., 1994. Tcl and the Tk Toolkit. ISBN 0-201-63337-X, Addison-Wesley, USA.
- Schäffer H. A. and Klopman G., 1997. Review of multidirectional active wave absorption methods. In: *Proceedings of the I.A.H.R. seminar on multidirectional waves and their interaction with structures, 27<sup>th</sup> I.A.H.R. congress, San Francisco, USA, pp.159-182.*
- Torrey M.D., Cloutman L.D., Mjolsness R.C., Hirt C.W., 1985. NASA-VOF2D: a computer program for incompressible flows with free surfaces. Report LA-10612-MS, Los Alamos Scientific Report, Los Alamos, New Mexico, USA.
- Troch P., 1997. VOFbreak<sup>2</sup>, a numerical model for simulation of wave interaction with rubble mound breakwaters. In: *Proceedings 27<sup>th</sup> IAHR Congress, San Francisco, USA, pp. 1366-1371.*

Troch P. and De Rouck J., 1998. An Active Wave Generating-Absorbing Boundary Condition for VOF type numerical model. Submitted for Coastal Engineering.

Troch P., De Somer M., De Rouck J., Van Damme L., Vermeir D., Martens J.P., 1996. Wave attenuation inside a rubble mound breakwater based on full scale measurements. Proc. ICCE '96, Orlando, USA.

van der Meer J.W., Petit H.A.H., van den Bosch P., Klopman G., Broekens R.D., 1992. Numerical simulation of wave motion on and in coastal structures. In: Proceedings 23<sup>rd</sup> International Conference on Coastal Engineering, Venice, Italy, Vol.2, pp. 1772-1784.